International Journal of Mechanical and Production Engineering Research and Development (IJMPERD)
ISSN (P): 2249–6890; ISSN (E): 2249–8001
Vol. 9, Issue 6, Dec 2019, 707–724

FORMULAE TO PREDICT HOOP STRESSES ALONG THE TRANSVERSE XY PLANE OF A SMALL RADIAL CIRCULAR CROSS BORE IN THICK CYLINDERS

P. K. NZIU & L. M. MASU

Department of Mechanical Engineering, Vaal University of Technology, Vanderbijlpark, South Africa

ABSTRACT

This study developed an analytical formula to determine elastic hoop stresses in a radial circular cross bore along the transverse XY plane in closed thick cylinders under internal pressure. The developed formula was validated using a three dimensional finite element analysis. The developed hoop stress equation was able to predict fairly accurate the magnitudes of hoop stresses along the cross bore transverse edge in 12 out of 21 models studied. Further, this formula was found to predict correctly the hoop stresses at the intersection of the main bore and the cross bore in 6 models.

KEYWORDS: Radical Circular, Thick Cylinders & Cross Bore

Received: Aug 15, 2019; **Accepted:** Sep 05, 2019; **Published:** Nov 18, 2019; **Paper Id.:** IJMPERDDEC201960

Original Article

INTRODUCTION

Cross bores are holes or openings that are constructed on the wall of thick cylinder to provide provision for fitting essential operation and maintenance accessories (Nziu and Masu, 2019a). Whenever these cross bores are positioned at the centroidal axis of the cylinder are termed as being radial. The most commonly used cross bore shapes in the design of thick cylinders are either circular or elliptical. For circular cross bores, whenever the ratio of the cross bore to main bore diameter is ≤ 0.5 is termed as being small. On the other hand, a cross bore is referred as being large when the aforesaid bore ratio is >0.5 (Nziu and Masu, 2019b). Unfortunately, introduction of any form of cross bores in the design of thick cylinders results in tremendous increase of hoop stress magnitudes. This high magnitude of hoop stress leads to reduction in pressure carrying capacity by nearly 60% (Nziu, 2018).

In case of radial circular cross bores, the magnitude of hoop stress along the cross bore transverse plane is presumed to be maximum. Besides, most analytical formulae used in the design of cross bored thick cylinders are only able to predict hoop stress at the intersection between the cross bore and the main bore. Though, other studies have reported that maximum hoop stress does not necessarily occur at the cross bore intersection, but slightly away from the cross bore intersection along the transverse plane (Nziu and Masu, 2019c). Therefore, this study developed an analytical formula that can predict magnitudes of elastic hoop stresses along the transverse edge of the cross bore in closed thick cylinders.

Analytical Derivation of Elastic Stresses along a Radial Circular Cross Bore in a Thick walled Cylinder

This section of the study dealt with the analytical derivation of hoop stresses along the radial circular cross bore in a thick walled cylinder with closed ends. Figure 1 illustrates the main bore and the cross bore configuration including the associated stresses. The global coordinates of the configuration are indicated by the direction of the principal stresses in the main cylinder. Whereas, the local coordinates are indicated by the direction of stresses in the cross bore.

The derivation took an account of four states of stresses acting in a closed cylinder when both the main bore and the cross bore are subjected to internal pressure. These various states of the stresses are discussed in the following four subsections.

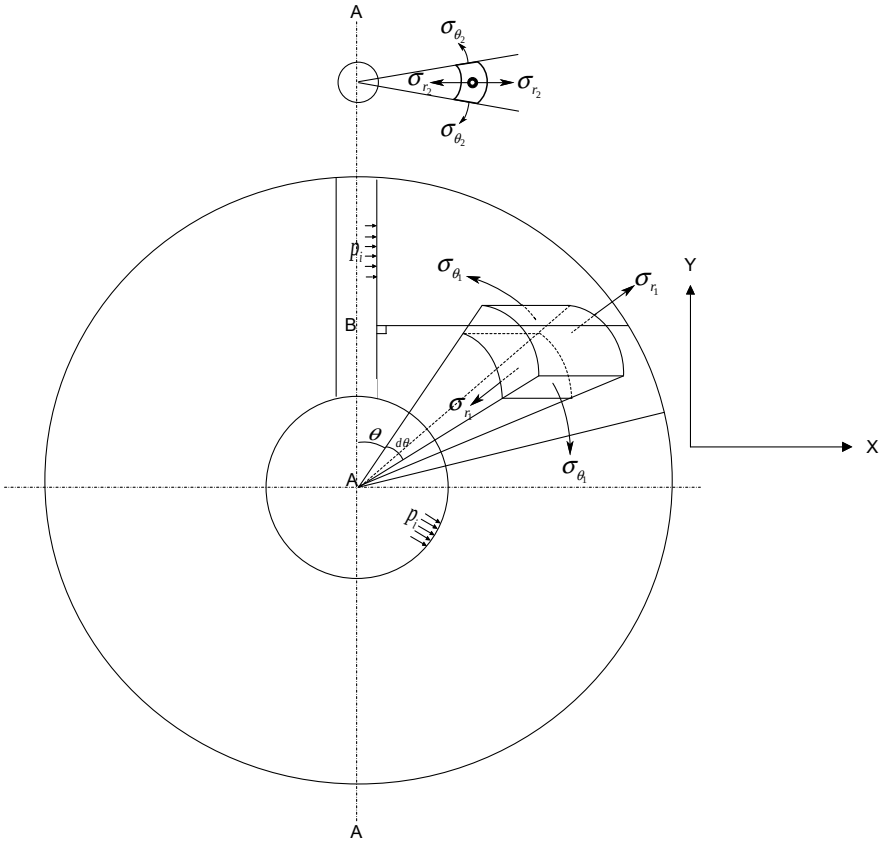

Figure 1: Main Bore – Cross Bore Configuration.

where; p_i is the internal pressure, σ_{θ_1} is the hoop stress generated by the pressurised main bore, σ_{r_1} is the radial stress generated by the pressurised main bore, $d\theta$ is the angle subtended by the small element and θ is the angle between the vertical axis and the small element.

Stresses in a Thick Walled Cylinder without a Cross Bore (Step 1)

In this step, the stresses that exist in a thick walled cylinder without a cross bore were calculated using Lame's theory. The hoop σ_{θ_1}, radial σ_{r_1} and axial $\sigma_z$stresses in a closed thick-walled cylinder without a cross bore subjected to an internal pressure p_i are given by equations 1, 2 and 3, respectively.

$$\sigma_{\theta_1} = \frac{p_i}{K^2 - 1}\left(1 + \left(\frac{R_0}{R}\right)^2\right), \text{ and} \quad (1)$$

$$\sigma_{r_1} = \frac{p_i}{K^2 - 1}\left(1 - \left(\frac{R_0}{R}\right)^2\right) \quad (2)$$

$$\sigma_z = \frac{P_i}{K^2 - 1} \quad (3)$$

where, K is the cylinder thickness ratio and R is the arbitrary radius measured from the main bore centre.

The configuration showing the introduction of a radial cross bore in the thick walled cylinder is illustrated in figure 1. The stresses induced by the cross bore were calculated by assuming the cross bore as an open ended cylinder. In addition, it was assumed that, the curvature of the cylinder had no effect on the stress concentration. The internal radius of the cross bore was denoted as r_i. Whereas, the external radius which was defined as the horizontal distance between the transverse plane of the cross bore and the outside surface of the main cylinder was denoted as b, as shown in figure 2. Along the outside surface of the cylinder, the external radius b is given by $R_0 \sin\theta$.

The corresponding hoop, σ_{θ_2} and the radial, σ_{r_2} stresses were obtained by assuming the Lame's theory along the pressurised cross bore. To calculate the lame's theory constants, the following boundary conditions were used. At the inside surface of the cross bore, $r = r_i$, the corresponding radial stress $\sigma_{r_2} = -p_i$. Whereas, at the outside surface of the vessel, $r = R_0 \sin\theta$, the corresponding radial stress $\sigma_{r_2} = 0$. From which, the corresponding stresses are calculated using equations 4 and 5.

$$\sigma_{\theta_2} = \frac{P_i r_i^2}{R_0^2 \sin^2\theta - r_i^2}\left(1 + \left(\frac{R_0 \sin\theta}{r}\right)^2\right) \tag{4}$$

$$\sigma_{r_2} = \frac{P_i r_i^2}{R_0^2 \sin^2\theta - r_i^2}\left(1 - \left(\frac{R_0 \sin\theta}{r}\right)^2\right) \tag{5}$$

$K = \frac{R_0}{R_i}$ and $m = \frac{R_i}{r_i}$, r_i can be written as $r_i = \frac{R_0}{Km}$

Therefore, substituting these afore mentioned expressions in equations 4 and 5 and solving, they became;

$$\sigma_{\theta_2} = \frac{k^2 m^2 p_i}{k^4 m^4 \sin^2\theta - 1}\left(1 + \frac{R_0^2}{R^2}\right) \tag{6}$$

$$\sigma_{r_2} = \frac{k^2 m^2 p_i}{k^4 m^4 \sin^2\theta - 1}\left(1 - \frac{R_0^2}{R^2}\right) \tag{7}$$

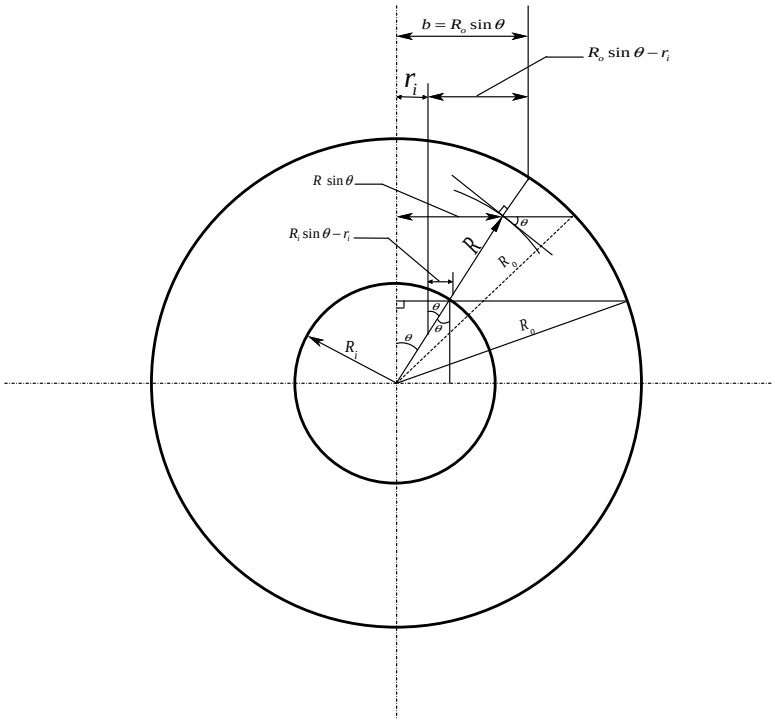

Figure 2: Cross Bore Configuration.

Stresses Induced by the Axial Tensile Stress due to the Closed Ends on the Main Bore Cylinder (Step 3)

Axial tensile stress is generated uniformly across the thickness of the cylinder due to the closed ends. Figure 3 shows the configuration of the axial tensile stress in a cross bore thick walled cylinder. The local coordinates are indicated by the direction of stress as shown in figure 3.

The solution for this configuration was aided by considering an imaginary cylinder of radius R_i, which is represented by the dotted ring as shown in Figure 3. Assuming an elastic system, the total radial stress around the cross bore was found to be composed of two parts (Faupel and Harris, 1957; Gerdeen, 1972; Hearn, 1999).

The first part entailed stress due to the internal pressure which was considered as a constant radial stress. While, the second part comprised of sinusoidal stress variation, signifying the variation of radial stress across the wall thickness. This form of stress variation represented the required surface stresses at the cross bore, to give the same internal stresses that are present in a similar cylinder without a cross bore (Gerdeen, 1972). Thus, the second part was considered as consisting of a varying radial stress. As a result, the two parts were solved independently as shown in the following section, Steps 3a and 3b.

Stresses Induced by a Constant Radial Stress at the Cross Bore (Step 3a)

The stresses induced by a constant radial stress at the cross bore were calculated by considering the region between the two circular rings, of radii r_i and R_i, as illustrated in figure 3. Ignoring the effects of the curvature in the main cylinder, the stresses within the two rings correspond to those existing in a thick walled cylinder (Ford and Alexander, 1977).

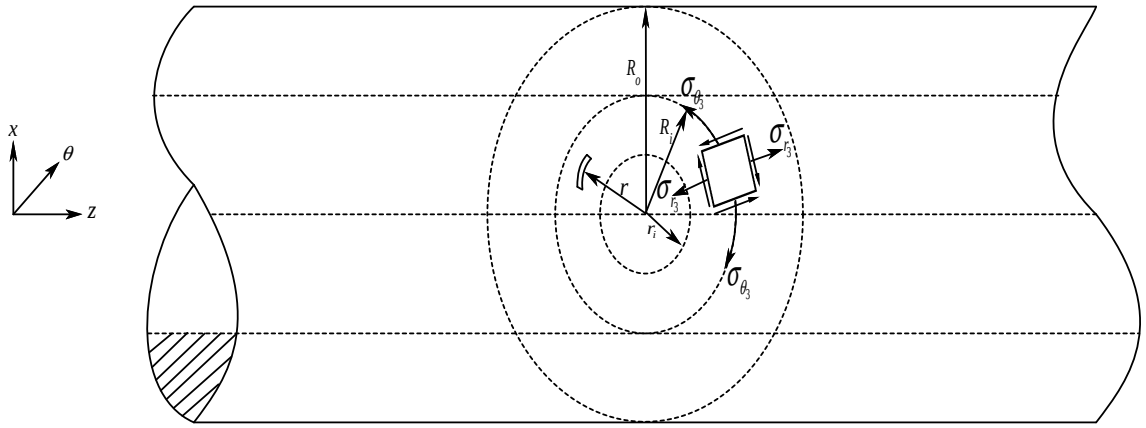

Figure 3: Configuration of the Axial Tensile Stress in a Cross Bored Vessel.

Thus, the Lame's equation was applied within the two rings, formed by radii r_i and R_i. The corresponding hoop $\sigma_{\theta_{3a}}$and radial $\sigma_{r_{3a}}$stresses were obtained by applying radial stress boundary conditions. At the inner surface of the cross bore $r = r_i$, the corresponding radial stress $\sigma_{r_{3a}} = -p_i$. Whereas, on the outer ring, $r = R_i$ (which also coincides with the inner surface of the main bore), the corresponding radial stress $\sigma_{r_{3a}} = \sigma_z$. Hence, the contributions to the hoop and radial stresses are shown by equations 8 and 9.

$$\sigma_{\theta_{3a}} = \frac{1}{m^2 - 1}\left[m^2\sigma_z + p_i + m^2 \frac{R_i^2}{r^2}(\sigma_z + p_i) \right], \quad \text{and (8)}$$

$$\sigma_{r_{3a}} = \frac{1}{m^2 - 1}\left[m^2\sigma_z + p_i - m^2 \frac{R_i^2}{r^2}(\sigma_z + p_i) \right] \quad (9)$$

Stress Induced by the Varying Radial Stress (Step 3b)

The stress distribution induced by the sinusoidal stress variation was solved using the theory of elasticity and stress functions methods (Gerdeen, 1972; Faupel and Fisher, 1981). The trend of the radial and shear stress variation that simulates the stress behaviour present in a similar cylinder without a cross bore was established in the form of polar coordinates (Hearn 1999). At the outer ring, $r = R_i$, which also coincides with the surface of the cylinder bore, the radial stress $\sigma_{r_{3b}}$ is $\frac{1}{2}\sigma_z \cos 2\theta$. Whereas, the corresponding shear stress $\tau_{r\theta_{3b}}$at the same position is $-\sigma_z \sin 2\theta$. Several authors (Timoshenko and Goodier 1951, Geerden 1972, Ford and Alexander 1977, Faupel and Fisher 1981 and Hearn 1999) have classified the stress function formed under these conditions as an axisymmetric biharmonic order. Because the harmonic order denoted the solution as n is equal to 2. This trend, therefore, justified the use of the following biharmonic stress function equation φ.

$$\varphi = (Cr^2 + D/r^2 + Er^4 + F)\cos 2\theta. \quad (10)$$

The three corresponding stress components generated from this biharmonic stress function, as cited by the authors mentioned in the preceding paragraph were calculated as follows;

$$\sigma_{r_{3b}} = -\left(2C + \frac{6E}{r^4} + \frac{4F}{r^2}\right)\cos 2\theta \quad (11)$$

$$\sigma_{\theta_{3b}} = \left(2C + 12Dr^2 + \frac{6E}{r^4}\right)\cos 2\theta \quad (12)$$

$$\tau_{r\theta_{3b}} = \left(2C + 6Dr^2 - \frac{6E}{r^4} - \frac{2F}{r^2}\right)\sin 2\theta \quad (13)$$

The four constants C, D, E and F, were evaluated by considering the following boundary conditions obtained using radial and shear stresses.

- With reference to figure 3, at the surface of the cross bore, $r = r_{i,}$ the corresponding radial stress$\sigma_{r_{3b}} = -p_i$. Specifically, the radial stress on the cross bore surface is equal to the gauge pressure and acts in the opposite direction. Substituting these boundary conditions into equation 11,

  $-p_i = -\left(2C + \frac{6E}{r_i^4} + \frac{4F}{r_i^2}\right)\cos 2\theta$, which can be re-written as

  $$p_i \sec 2\theta = 2C + \frac{6E}{r_i^4} + \frac{4F}{r_i^2} \quad (14)$$

- With reference to figure 2, the magnitude of both the radial and the shear stress at the outer surface of the cylinder when the radius $r = b$, is zero. Thus, the expressions for radial and shear stress can be formulated. Using equation 11, the following radial stress equation was formulated.

  $$0 = -\left(2C + \frac{6E}{b^4} + \frac{4F}{b^2}\right)\cos 2\theta$$

As seen from the preceding expression, the product of the two terms in the right hand side is equal to zero. However, the magnitude of $\cos 2\theta$ varies along the outer surface of the cylinder. Thus, its magnitude is not equal to zero at all points along the surface. Therefore, the first term is equal to zero. Hence,

$$0 = -\left(2\mathrm{C} + \frac{6\mathrm{E}}{\mathrm{b}^4} + \frac{4\mathrm{F}}{\mathrm{b}^2}\right) \quad (15)$$

Using the same analogy as discussed in the preceding paragraph, the expression for the shear stress was formulated using equation 13 as follows;

$$0 = \left(2\mathrm{C} + 6\mathrm{Db}^2 - \frac{6\mathrm{E}}{\mathrm{b}^4} - \frac{2\mathrm{F}}{\mathrm{b}^2}\right)\sin 2\theta$$

Similarly, the magnitude of $\sin 2\theta$ varies along the outer surface of the cylinder. Therefore, the term $\sin 2\theta \neq 0$ at all the points on the cylinder surface. Hence,

$$0 = \left(2\mathrm{C} + 6\mathrm{Db}^2 - \frac{6\mathrm{E}}{\mathrm{b}^4} - \frac{2\mathrm{F}}{\mathrm{b}^2}\right) \quad (16)$$

- With reference to Figure 3, at the outer ring, the radius $r = R_i$, (which also coincides with the inner surface of the cylinder bore), the corresponding shear stress$\tau_{r\theta_{3b}} = -\sigma_z \sin 2\theta$. Substituting these boundary conditions into equation 13.

  $$-\sigma_z = 2\mathrm{C} + 6\mathrm{DR_i}^2 - \frac{6\mathrm{E}}{\mathrm{R_i^4}} - \frac{2\mathrm{F}}{\mathrm{R_i^2}} \quad (17)$$

The aforementioned four equations formed from the boundary conditions are sufficient to solve for the unknown

constants C, D, E and F. They are presented inform of a matrix as shown in equation 18 hereafter.

$$\begin{bmatrix} 2 & 0 & \frac{6}{r_i^4} & \frac{4}{r_i^2} \\ -2 & 0 & -\frac{6}{b^4} & -\frac{4}{b^2} \\ 2 & 6b^2 & -\frac{6}{b^4} & -\frac{2}{b^2} \\ 2 & 6R_i^2 & -\frac{6}{R_i^4} & -\frac{2}{R_i^2} \end{bmatrix} \begin{bmatrix} C \\ D \\ E \\ F \end{bmatrix} = \begin{bmatrix} P_i \sec 2\theta \\ 0 \\ 0 \\ -\sigma_z \end{bmatrix} \tag{18}$$

The constants from this matrix expression were solved using Cramer's rule with the aid of computer mathematical software, Mathcad Version 15. The solutions of the constants are as follows;

$$\mathrm{C} = \frac{P_i R_i^6 r_i^4 + 2\sigma_z \cos 2\theta R_i^4 b^6 - 2\sigma_z \cos 2\theta R_i^4 b^4 r_i^2 + P_i R_i^2 b^4 r_i^4 - 2P_i b^6 r_i^4}{2\cos 2\theta (R_i - b)(R_i + b)(b - r_i)(b + r_i)\left(3R_i^4 b^2 - R_i^4 r_i^2 + R_i^2 b^4 - R_i^2 b^2 r_i^2 - 2b^4 r_i^2\right)} \tag{19}$$

$$\mathrm{D} = \frac{-2\mathrm{P_I R_i^4 r_i^4} - 3\mathrm{P_i b^4 r_i^4} + 2\mathrm{P_i R_i^2 b^2 r_i^4} + 3\mathrm{R_i^4 b^4 \sigma_z \cos 2\theta} - 4\mathrm{R_i^4 b^2 r_i^2 \sigma_Z \cos 2\theta} + R_i^4 r_i^4 \sigma_z \cos 2\theta}{6\cos 2\theta(\mathrm{R_i - b})(\mathrm{R_i + b})(\mathrm{b - r_i})(\mathrm{b + r_i})\left(3\mathrm{R_i^4 b^2 - R_i^4 r_i^2 + R_i^2 b^4 - R_i^2 b^2 r_i^2 - 2b^4 r_i^2}\right)} \tag{20}$$

$$E = \frac{R_i^2 b^4 r_i^2 \left(3P_i R_i^4 r_i^2 - P_i b^4 r_i^2 - 2P_i R_i^2 b^2 r_i^2 + 2R_i^2 b^4 \sigma_z \cos 2\theta - 2R_i^2 b^2 r_i^2 \sigma_z \cos 2\theta\right)}{6\cos 2\theta(\mathrm{R_i - b})(\mathrm{R_i + b})(\mathrm{b - r_i})(\mathrm{b + r_i})\left(3\mathrm{R_i^4 b^2 - R_i^4 r_i^2 + R_i^2 b^4 - R_i^2 b^2 r_i^2 - 2b^4 r_i^2}\right)} \tag{21}$$

$$\mathrm{F} = \frac{b^2\left(72P_i b^6 r_i^4 - 144P_i R_i^6 r_i^4 + 72P_i R_i^4 b^2 r_i^4 - 72R_i^4 b^6 \sigma_z \cos 2\theta + 72{R_i}^4 b^2 r_i^4 \sigma_z \cos 2\theta\right)}{\cos 2\theta\left(432R_i^6 b^4 - 576R_i^6 b^2 r_i^{23} + 144R_i^6 r_i^4 - 288R_i^4 b^6 + 288R_i^4 b^4 r_i^2 - 144R_i^2 b^8 + 144R_i^2 b^4 r_i^4 + 288b^8 r_i^2 - 288b^6 r_i^4\right)} \tag{22}$$

Stresses due to the Internal Pressure at the Cross Bore (Step 4)

Stress distribution due to the internal pressure at the cross bore was considered to be acting inside a thick walled cylinder with an infinite external radius, since the cylinder wall is "joined on itself" (Fessler and Lewin, 1956; Geerden , 1972; Ford and Alexander, 1977). Applying the Lame equation on the configuration shown in Figure 2 and assuming an infinite external radius, that is, $b \to \infty$.

$$\sigma_{\theta_4} = \frac{p_i}{\left(1 - \frac{r_i^2}{b^2}\right)}\left(1 + \frac{r_i^2}{b^2}\right) \to p_i, \text{ and} \tag{23}$$

$$\sigma_{r_4} = -\frac{p_i}{\left(1 - \frac{r_i^2}{b^2}\right)}\left(1 - \frac{r_i^2}{b^2}\right) \to -p_i \tag{24}$$

Superposition of Stresses at the Cross Bore Surface

The total hoop stress$\sigma_{\theta_{Total}}$ component in the hoop direction of the main cylinder along the transverse plane of the cross bore, which can also be taken as the maximum principal stress, was obtained by the summation of the corresponding hoop equations, in all the four cases considered , $\sigma_{\theta_{Total}}$.

$$= \frac{p_i}{k^2 - 1}\left(1 + \left(\frac{R_0}{R}\right)^2\right) + \frac{k^2 m^2 p_i}{k^4 m^4 \sin^2\theta - 1}\left(1 + \frac{R_0^2}{R^2}\right) + \frac{1}{m^2 - 1}\left[m^2 \sigma_z + p_i + m^2 \frac{R_i^2}{r^2}\left(\sigma_z + p_i\right)\right] +$$

$$\left(2C + 12Dr^2 + \frac{6E}{r^4}\right)\cos 2\theta + p_i \tag{25}$$

Three Dimensional Finite Element Analysis

Finite element analyses were performed on similar thick closed cylinders with radial cross bores using Abaqus version 6.16 commercial software program in order to validate equation 25. The modelling procedure followed in this work is detailed in Nziu (2018).

Seven cross bored cylinders with thickness ratios (K) 1.4, 1.5, 1.75, 2.0, 2.25, 2.5 and 3.0 were studied. In all the analyses, the main bore diameter of the cylinder was kept constant at 0.05 m. In this work, only results of small radial cross bores with size ratios (cross bore to main bore ratio) of 0.1, 0.3 and 0.5 were presented. The results were analysed along the cross bore transverse plane A-A, where$\theta = \frac{\pi}{2}$ (see Figure 1). Other studied cross bore size ratios were discussed elsewhere.

RESULTS AND DISCUSSIONS

Correlation of Analytical and Numerical Solutions

The magnitudes of hoop stress obtained by the analytical solution along the transverse edge of the radial cross bore were compared with their corresponding ones generated by finite element modelling. The numerical solution was selected as the reference method, since it had been authenticated. The selection of this reference method aided the calculation of error percentages between the two methods (Ford and Alexander, 1977). Since all the analyses were performed under elastic conditions, the results were presented per unit pressure for ease of comparison under the following subheadings.

Cross Bore to main Bore Ratio of 0.1

In this section, results of a high pressure vessel with main bore to cross bore size ratio of 0.1 are presented in figures 6–12; for thickness ratios, K = 1.4, 1.5, 1.75, 2.0, 2.25, 2.5 and 3.0.

From figures 6–12, it can be seen that the analytical method predicted lower stress values in comparison to those obtained by FEA. Notable disparity of the results given by analytical and numerical methods was seen in figures 6, 7 and 9. However, as the thickness ratio is increased, the solution given by the two methods began to converge, as illustrated by Figures 10 –12.With the exception of thickness ratios 1.4, 1.5 and 1.75, the magnitude of hoop stress was highest at the intersection between the cross bore and the main bore. However, the hoop stress reduced gradually along the cross bore depth. For K = 1.4, 1.5 and 1.75, the maximum hoop stress occurred slightly away from the intersection at approximately 1.25 mm.

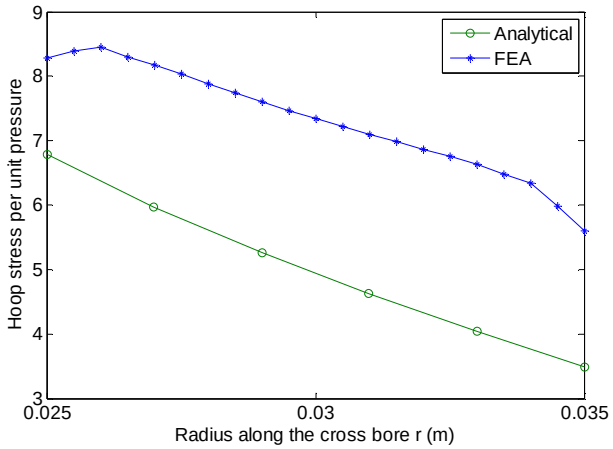

Figure 4: K = 1.4 CB = 0.1.

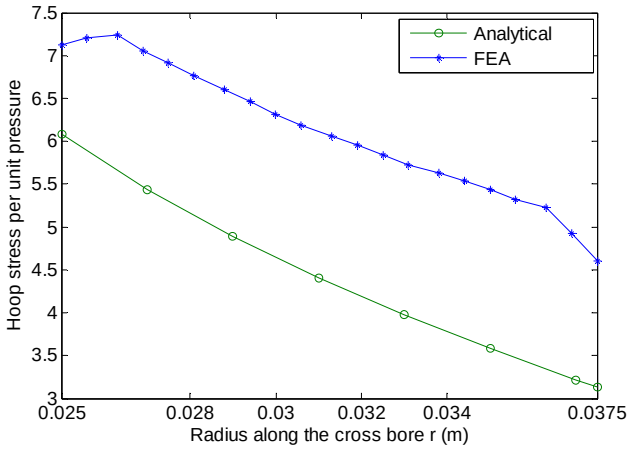

Figure 5: K = 1.5 CB = 0.1.

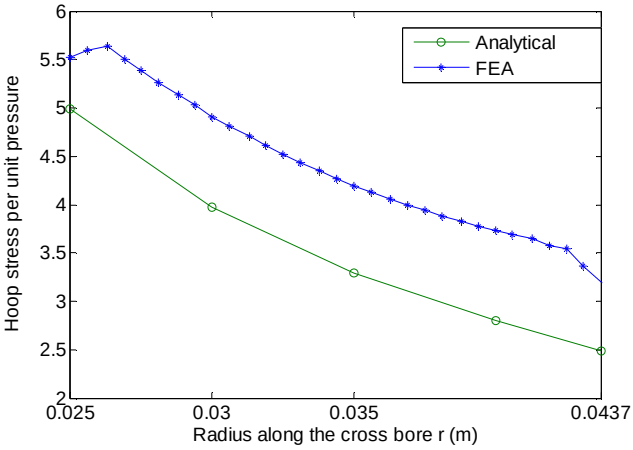

Figure 6: K = 1.75 CB = 0.1.

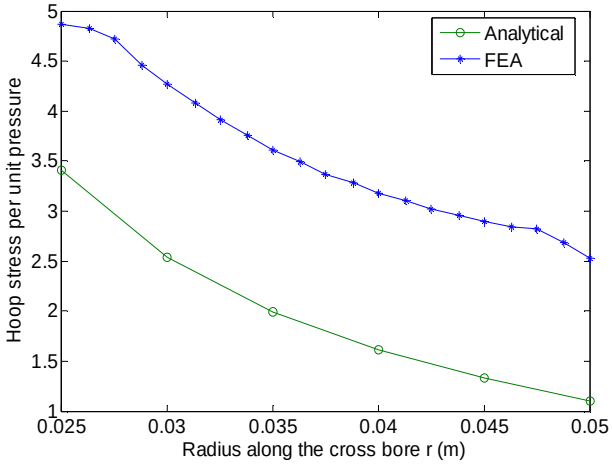

Figure 7: K = 2.0 CB = 0.1.

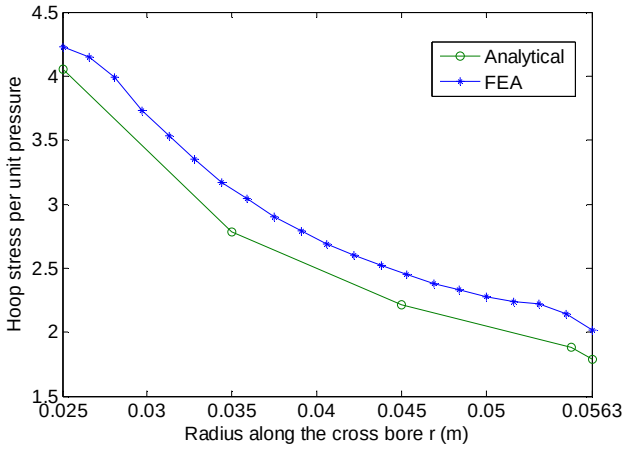

Figure 4: K = 2.25 CB = 0.1.

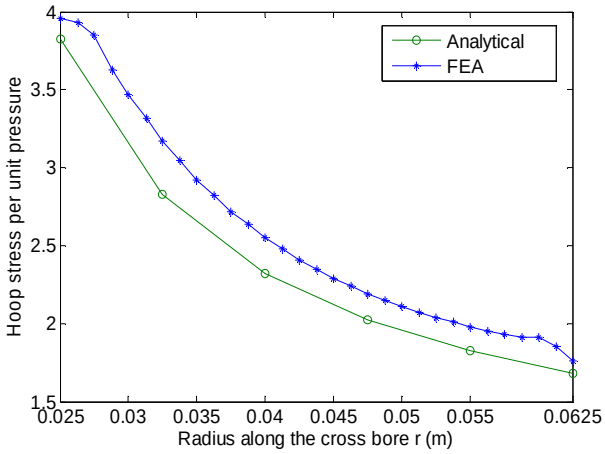

Figure 9: K = 2.5 CB = 0.1.

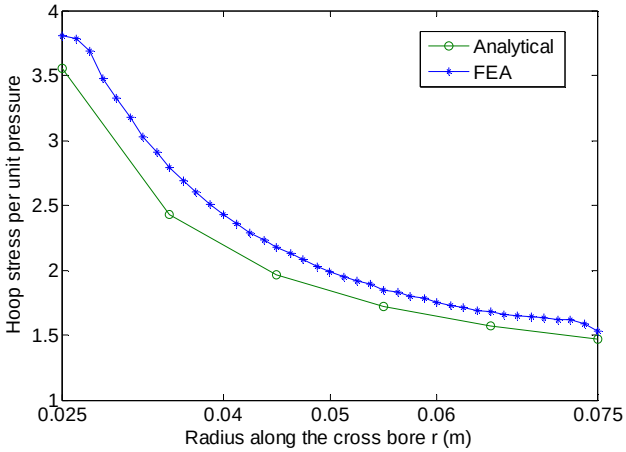

Figure 5: K = 3.0 CB = 0.1.

Respectively, these peaks were slightly higher by a margin of 2.13%, 1.63% and 3.96%, in comparison to those present at the intersection. This occurrence was attributed to redistribution of stress due to change in state of stress from plane stress to plane strain. Similar occurrence had previously been noted by Masu (1989) study.

A structure is termed to be under plane stress conditions whenever the magnitude of one of the three principal stresses is small in comparison to the other two stresses (Spyrakos, 1996). Usually, the magnitude of the small principal stress is approximated as zero. On the other hand, a structure is said to be under plane strain conditions whenever the strain developed along one of the principal axes is zero (Spyrakos, 1996). This phenomenon occurs as a result of one of the three sections of the structure being large in comparison to the other two sections.

The maximum value of hoop stress occurred in the pressure vessels with the smallest thickness ratio of K = 1.4. The peak values of the hoop stresses per unit pressure were at 6.783 and 8.460 for analytical and FEA methods, respectively. Whereas, the smallest magnitude of the hoop stress occurred in the cylinder with the highest thickness ratio, K = 3.0. This trend implied that the magnitude of hoop stress reduces with increase in the thickness ratio. Usually, as the thickness ratio increase the structural stiffness of the cylinder also increase, leading to lower hoop stresses and vice versa.

Comparing the results obtained through the analytical and FEA methods at the cross bore intersection, the lowest error was at 3.4% for K = 2.5. While the errors calculated from K = 2.25 and 3.0 were 4.1% and 6.4%, respectively. The other thickness ratios studied had errors above 9%.

A similar study conducted by Comleki *et al.* (2007) using FEA on thick cylinders having the same thickness ratio gave results that compared favourably to those obtained by the numerical solution, as tabulated in table 1.

Table 1: Hoop Stress Per Unit Pressure at the Intersection of Cross Bore Size Ratio of 0.1

K	1.4	1.5	1.75	2.0	2.25	2.5
Comleki *et al.* (2007) (FEA)	8.50	7.31	5.77	5.05	4.64	4.39
Present study (FEA)	8.29	7.12	5.52	4.87	4.23	3.96

The margin of error was computed by comparing the two FEA solutions and taking the results from the present study as the reference. The errors for K = 1.4, 1.5, 1.75 and 2.0 were found to be 2.6%, 2.6%, 4.4% and 3.7%, respectively. Interestingly, only the errors given by K = 2.25 and 2.5 were slightly higher at 9.6% and 10.1%. A condition attributed to the degree of mesh refinement during modelling. Usually, the Abaqus commercial software used in this study has better capability in control of element meshing than ANSYS software used in the Comleki *et al.* (2007) study. The good results correlation between the two studies further authenticated the modelling procedures adopted in this study.

Geerden (1972) performed analytical studies on pressure vessels with a cross bore size ratio of 0.1, having thickness ratios of K = 1.5, 2 and 3. The Geerden study predicted much higher hoop stresses at the cross bore intersection than those from the analytical and numerical results presented in this study. Errors exceeding 16% were noted. Probably, this large error margins were due to the inclusion of shear stresses in Geerden's solution during the computation of the hoop stress.

Cross Bore to Main Bore Ratio of 0.3

Results of a high pressure vessel with main bore to cross bore size ratio of 0.3 are presented in figures 13 –19 for K = 1.4, 1.5, 1.75, 2.0, 2.25, 2.5 and 3.0.

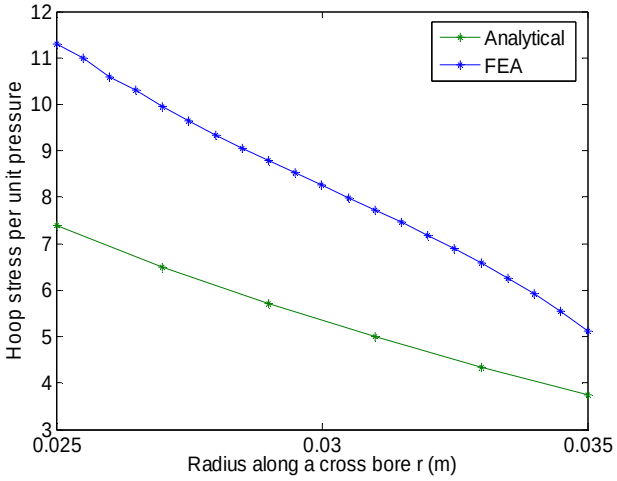

Figure 6: K = 1.4 CB = 0.3.

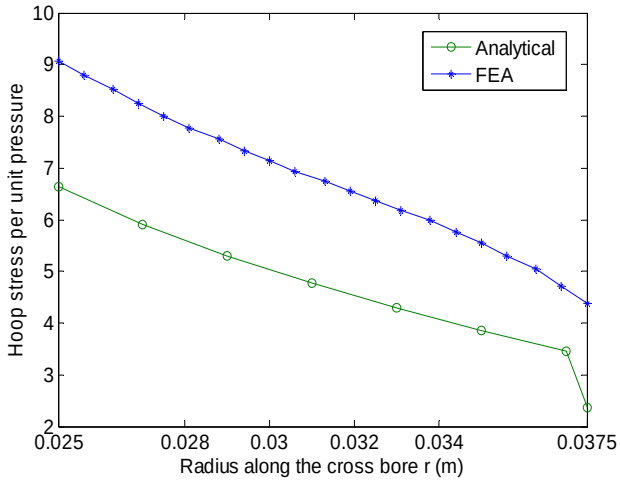

Figure 7: K = 1.5 CB = 0.3.

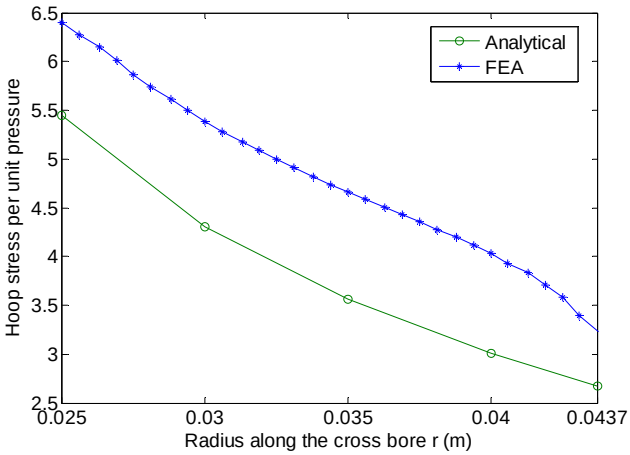

Figure 8: K = 1.75 CB = 0.3

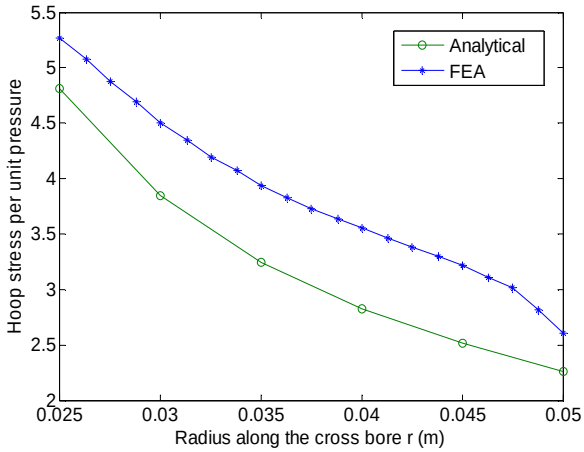

Figure 9: K = 2.0 CB = 0.3

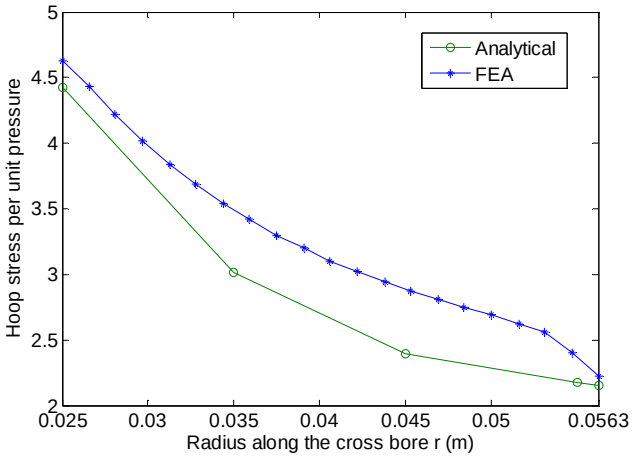

Figure 10: K = 2.25 CB = 0.3.

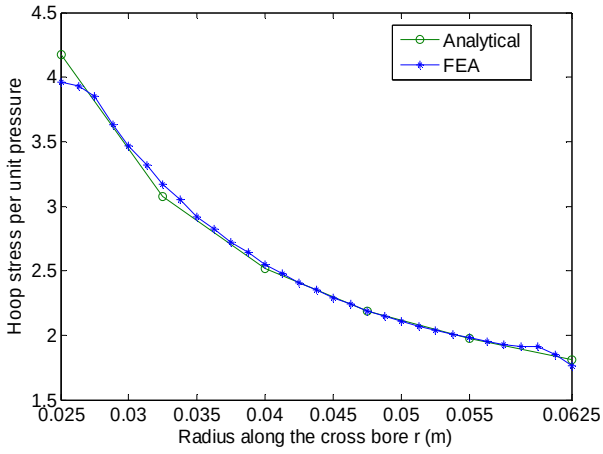

Figure 11: K = 2.5 CB = 0.3.

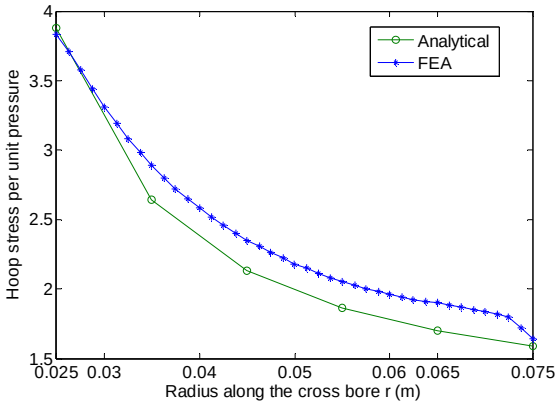

Figure 12: K = 3.0 CB = 0.3.

In this section, a similar stress distribution pattern as previously exhibited in the previous section was observed. The magnitudes of hoop stresses were high at the cross bore intersection and reduced gradually towards the outside surface of the cylinder.

A general comparison between hoop stresses due to the introduction of the cross bore size ratio of 0.3 and those of 0.1, as illustrated in figures 6–19, showed an increase in magnitude of hoop stress as the cross bore size increased. For instance, in the case of K = 1.4, the hoop stress per unit pressure at the intersection was found to be 7.405 and 11.34, for analytical and FEA, respectively. Resulting to an increase of 9.17% and 36.9% when compared with similar stresses obtained in pressure vessels with a cross bore size ratio of 0.1 presented earlier in preceding section. Usually, the structural stiffness of the cylinder reduces with the increase of the cross bore size leading to higher hoop stresses.

The disparities in hoop stress distribution predicted by the analytical and FEA were more pronounced in K = 1.4, 1.5 and 1.75 as shown in figures 13–15. However, as the thickness ratio increased, the hoop stress distribution curves generated by both the analytical and numerical methods tended to converge.

Comparing the results given by the two methods, the minimal error was at 1.15% for K = 3.0, while, the thickness ratios of K = 2.0, 2.25 and 2.5 gave errors of 1.97%, 4.37% and 8.62%, respectively. The margin of error presented by other thickness ratios exceeded 15%. It was noted that the margin of error increased tremendously with reduction in thickness ratio.

Geerden (1972) carried out similar studies on pressure vessels with a radial cross bore size ratio of 0.3. The results by Geerden (1972) at the cross bore intersection are compared in Table 2 with corresponding ones obtained in the present study.

Table 2: Hoop Stress Per Unit Pressure at the Intersection of Cross Bore Size Ratio of 0.3

K	1.5	2.0	3.0
Geerden, 1972 (Analytical)	7.98	5.43	4.16
Present study (Analytical)	6.63	4.81	3.88
Present study (FEA)	9.07	5.27	3.83

Errors of 20.3%, 12.7% and 7.35%, for K = 1.5, 2.0 and 3.0 respectively were obtained upon comparison with the analytical solution presented in this study. Correspondingly, errors calculated upon comparison with FEA data were 12%, 3% and 8.58% for K = 1.5, 2.0 and 3.0, respectively. Thus, only the FEA results for K = 2 were within the acceptable margin of error.

Cross Bore to Main Bore Ratio of 0.5

Results of a high pressure vessel with main bore to cross bore size ratio of 0.5 are presented in figures 20 –26 for K = 1.4, 1.5, 1.75, 2.0, 2.25, 2.5 and 3.0.

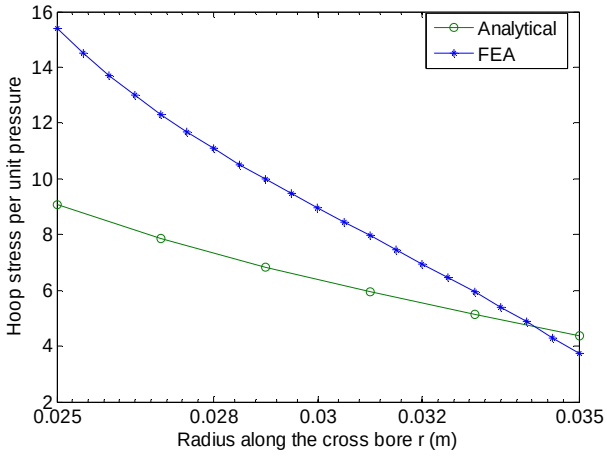

Figure 18: K =1.4 CB = 0.5.

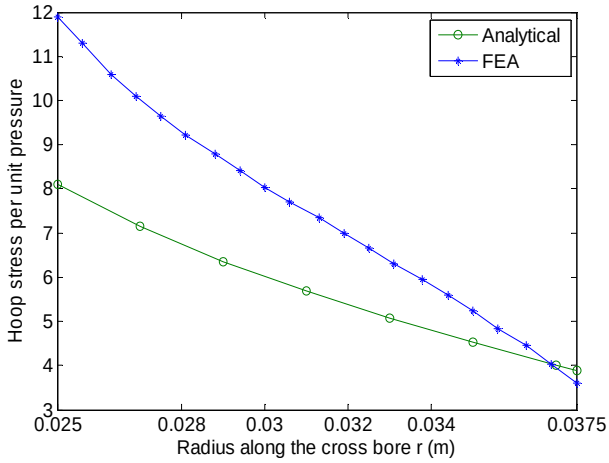

Figure 13: K = 1.5 CB = 0.5.

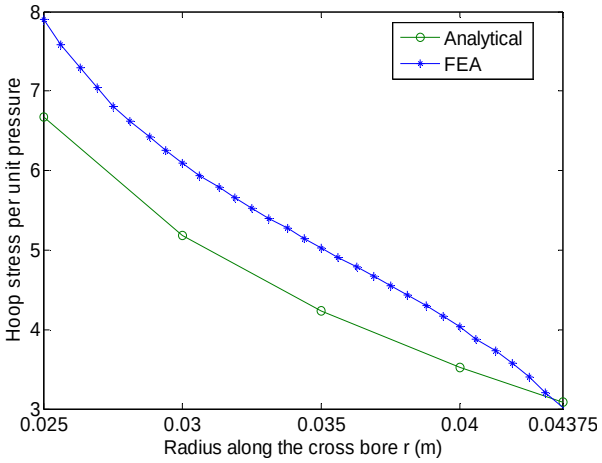

Figure 14: K = 1.75 CB = 0.5.

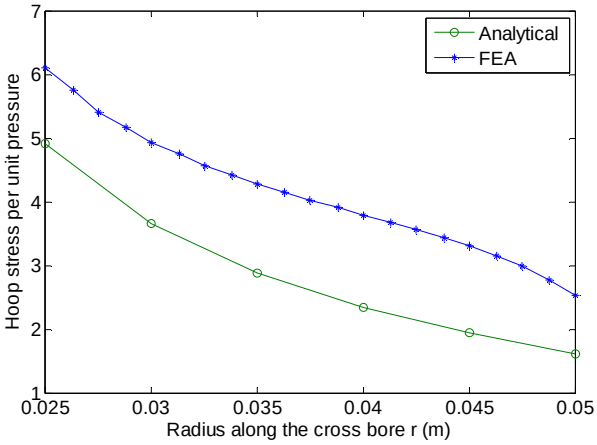

Figure 15: K = 2.0 CB = 0.5.

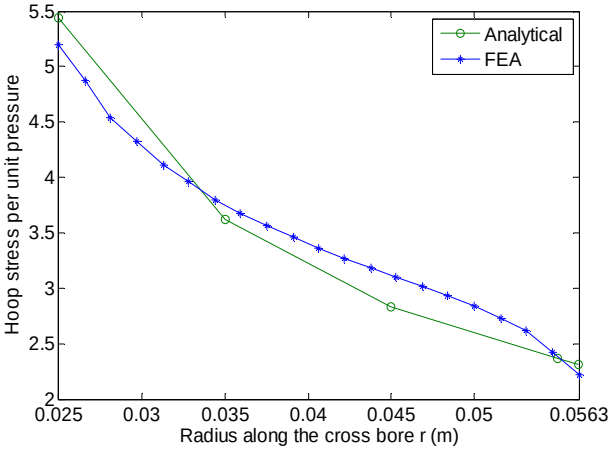

Figure 16: K = 2.25 CB = 0.5

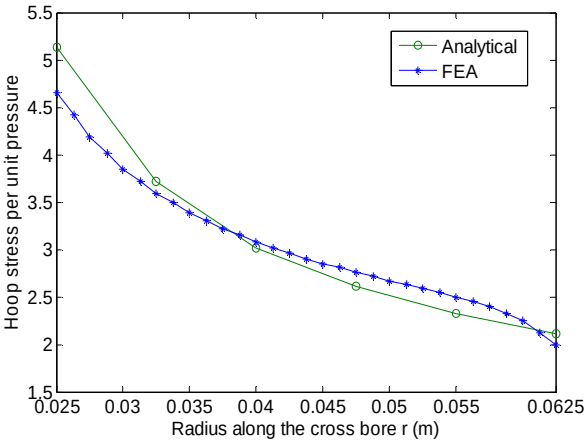

Figure 17: K = 2.5 CB = 0.5

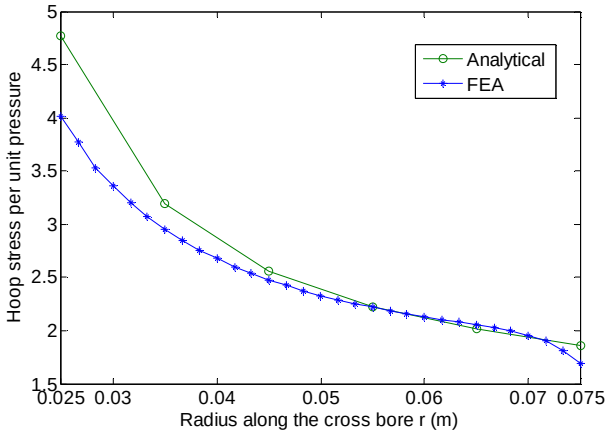

Figure 18: K = 3.0 CB = 0.5.

Notable variation in stress distribution between the two methods were seen in K = 1.4 and 1.5, as illustrated in Figures 20 and 21. However, as the thickness ratio increased, a significant reduction in the disparities was noted. The stress distribution predicted by the FEA was higher than that of the analytical method at the cross bore intersection. Nevertheless, FEA predicted lower hoop stresses than the analytical method towards the outer surface of the cylinder.

The hoop stress at the cross bore intersection was maximum in the cylinder with thickness ratio K = 1.4. In the same thickness ratio, a comparison between cross bore size ratio of 0.3 and that of 0.5 at the cross bore intersection, as shown in figures 13 and 20, indicated a rise in hoop stress by 22.5% for analytical and 35.5% for FEA analyses. This trend signified that the hoop stress increases with increase in the cross bore size. This observation further confirms that the structural stiffness of the cylinder reduces with increase in the cross bore size leading to high magnitude of hoop stresses. Comparing the results from the two methods presented in this study, acceptable margin of error of 3.3% and 5% were only obtained for the thickness ratios 2.0 and 2.25, respectively. The error margin given by other thickness ratios studied exceeded 11%.

Several studies Fessler and Lewin (1956), Faupel and Harris (1957) and Gerdeen (1972) have been done on radial cross bores, with a main bore to cross bore ratio of 0.5 in thick walled pressure vessels using both experimental and analytical methods. The comparison of results at the cross bore intersection from these studies with those of the present study is tabulated in table 3.

Table 3: Hoop Stress PerUnit Pressure at the Intersection of Cross Bore Size Ratio of 0.5

K		1.5	2.0	2.5	3.0
Fessler and Lewin (1956)	Analytical	-	-	-	3.53
Fessler and Lewin (1956)	Experimental	-	-	-	3.5
Faupel and Harris (1957)	Analytical	7.54	4.78	3.94	-
Faupel and Harris (1957)	Experimental	6.11	4.37	3.73	-
Gerdeen (1972)	Analytical	7.02	4.67	-	-
Present study	Analytical	8.11	5.91	5.14	4.77
Present study	FEA	11.95	6.11	4.65	4.02

Faupel and Harris (1957) performed both analytical and experimental analyses on pressure vessels with K = 1.5. They reported maximum hoop stresses per unit pressure of 7.54 and 6.11 for analytical and FEA analyses, respectively. Gerdeen (1972) carried out an analytical study on the same cross bore size and reported a hoop stress value of 7.02 at the intersection.

The findings of these two previous studies indicated slightly lower hoop stresses than those presented in this work. The closest prediction was at 7% error when calculated using the analytical results developed in the present study.

On cylinders with K = 2, Faupel and Harris (1957) gave hoop stresses per unit pressure at the intersection as 4.784 and 4.367 for analytical and experimental methods, respectively, while the analytical method by Geerden (1972) gave a hoop stress value at the cross bore intersection as 4.667. These two analytical solutions from previous studies compared favourably with those given by the analytical method in this study

In contrast, the results presented by Faupel and Harris (1957) for K = 2.5 gave lower hoop stresses of 3.936 and 3.729 for analytical and experimental methods. The minimum error obtained upon comparison with FEA data exceeded 19%.

Fessler and Lewin (1956) predicted hoop stress at the intersection using both analytical and experimental method for K = 3.0. The study gave the hoop stress per unit pressure at the intersection as 3.525 and 3.5 for both analytical and experimental methods, respectively. Interestingly, a similar analytical study by Geerden (1972) predicted the magnitude of hoop stress as 3.5625. However, when these results were compared with those of the present study, errors exceeding 12.8% were noted.

Another study by Ford and Alexander (1977) derived equation 26 for determining hoop stress in thick walled cylinder having small radial cross bore regardless of its size at the intersection of the main bore and the cross bore.

$$\frac{4K^2+1}{K^2-1}p_i \tag{26}$$

Since, for small cross bores, the main bore to cross bore maximum size ratio is 0.5. Therefore, the results given by the equation 26for cross bore size ratio of 0.5were compared with those presented in this study for the same ratio as shown in figure 27.

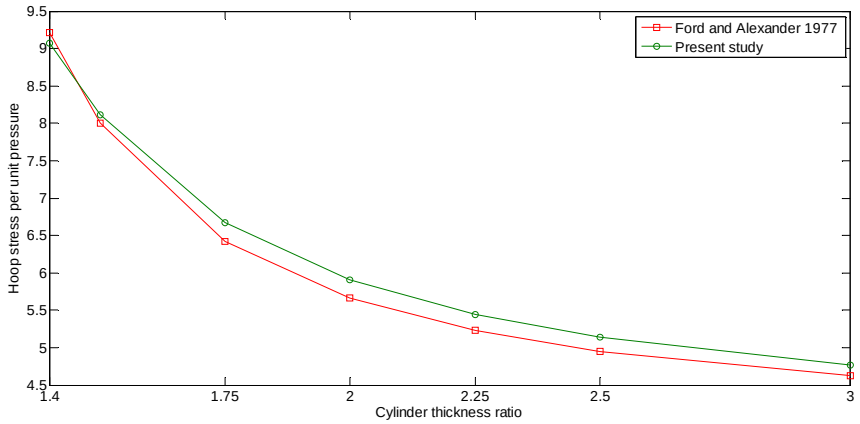

Figure 19: Comparison between Hoop Stress Generated by Equation 26 by Ford and Alexander (1977) and that obtained using Equation 25 developed in this study.

As illustrated in figure 27, the analytical results at the intersection presented by this study for cross bore size ratio of 0.5 were found to be in good agreement with those given by equation 26. The error was observed to increase slightly with increase in thickness ratio. This occurrence was attributed to different assumptions made during the development of these solutions. For instance, the study by Ford and Alexander (1977) assumed a biaxial stress field in their analysis.

In this study, the focus was mainly on the cross bore intersection, where stresses were high. Out of 21 studied models, the analytical solution correctly predicted the magnitude of the hoop stresses in 6 models at the cross bore intersection. In brief, for small cross bores, the total hoop stress along the cross bore in the cylinder is the sum of the hoop stresses in the main cylinder with a bore superimposed to the corresponding one generated by the pressurised cross bore when it is presumed to be acting alone. A preliminary numerical study was done arbitrarily on K = 3.0 having the smallest cross bore size of 0.1 to determine separately the magnitude of the hoop stress generated by the main cylinder and that of the cross bore. For the main cylinder, the internal pressure was applied at the inside surface of the cylinder only. Similarly, for the cross bore, the internal pressure was applied on the cross bore only. The hoop stress per unit pressure due to the separate loading was found to be 3.0 and 0.88 for the main cylinder and cross bore, respectively. Thus, the sum of the hoop stresses per unit pressure in the cylinder was 3.88. Therefore, the hoop stress generated by the main cylinder alone was 77.3%, while that of the cross bore was 22.7%. According to Ford and Alexander (1977) this superimposing phenomenon is true whenever the size of the cross bore size is small, because other factors such as Poisson's ratio have insignificant effects. Further comparison between maximum hoop stresses generated by the cross bored cylinder alone with that of a similar plain cylinder indicated an increase of hoop stress by 140%.

Moreover, the disparities in results resulting from analytical and numerical approaches were attributed to some of the assumptions made during the solution development and the limitations of the Abaqus software. For instance, in the development of the analytical solution it was assumed that the cylinder curvature has no effect on stress distribution. In addition, it was assumed that the axial stress was constant along the cross bore. This assumption of constant axial stress was contrary to the axial results presented by Nziu (2018) study. Nevertheless, the ability of the Abaqus software in predicting the stresses correctly at the surface was not confirmed. A numerical software suitable for the determination of surface stresses such as boundary integral element was recommended.

CONCLUSIONS

The developed stress equation was able to predict fairly accurate the magnitudes of hoop stresses along the cross bore transverse edge in 12 out of 21 models studied. Further, this formula was found to predict correctly hoop stresses at the intersection of the main bore and the cross bore in 6 models.

REFERENCES

1. *Faupel, J. H. and Fisher, F. E. (1981), "Engineering design- A synthesis of stress analysis and materials engineering", John Wiley and sons, Canada, ISBN 0-471-03381-2.*
2. *Faupel, J. H. and Harris, D. B. (1957)," Stress concentration in heavy-walled cylindrical pressure vessels", Industrial and engineering chemistry, Vol. 49, pp. 1979–1986.*
3. *Fessler, H. and Lewin, B. H. (1956), "Stress distribution in a tee-junction of thick pipes", British journal of applied physics, Vol. 7, pp. 76–79.*
4. *Rajashekhar, M., Reddy, K. R., & Goud, C. R. (2016). Study on validation of different IPM modules against bhendi shoot and fruit borer, Earias vittella. Int. J. Agric. Sci. Res, 6(3), 259–265.*
5. *Ford, H. and Alexander, J. (1977), "Advanced mechanics of materials", John wiley and sons inc., Canada, second edition.*
6. *Gerdeen J. C. (1972), "Analysis of stress concentration in thick cylinders with sideholes and crossholes", Trans. ASME, Journal Engineering Industry, No. 94, pp. 815–823.*

7. *Hearn, E. J. (1999), "Mechanics of materials 2", Butterworth-Heinemann, Great Britain, ISBN 0-7506 3266-6, Third edition.*
8. *Masu, L. M. (1989), "The effect of cross bore geometry on the strength of pressure vessels", PhD thesis, University of leeds.*
9. *Nziu, P. K. (2018), "Optimal geometric configuration of a cross bore in high pressure vessels", Doctorate thesis, Vaal University of Technology.*
10. *Osiński, P., & Cependa, P. Development of a method for determining micro-leaks and volumetric efficiency in pneumatic cylinders.*
11. *Nziu,P. K.andMasu, L. M. (2019a) , "Elastic strength of high pressure vessels with a radial circular cross bore", International journal of mechanical and production engineering research and development, Vol. 9, issue 3, pp. 1275–1284, doi: 10.24247/ijmperdjun2019133.*
12. *Nziu, P. K.andMasu, L. M. (2019b), "Cross bore geometry configuration effects on stress concentration in high pressure vessels. A review", International journal of mechanical and materials engineering, , Vol. 14, issue 6, doi: 10.1186/s40712-019-0101-x*
13. *Bodade, P. R., Jogi, N., Gorde, M., Paropte, R., & Waghchore, R. Use of Internal Threads of Different Pitches to Enhance Heat Transfer in A Circular Channel.*
14. *Nziu, P. K.andMasu, L. M. (2019c), "Formulae for predicting stress concentration factors in flat plates and cylindrical pressure vessels with holes; A review", International journal of mechanical and production engineering research and development, accepted for publication in August 2019.*
15. *PATEL, C. N., & Kishori, M. S. (2016). Analytical and Software Based Comparative Analysis of on Ground Circular Water Tank. International Journal of Civil Engineering (IJCE), 5(3).*
16. *Spyrakos, C. C. (1996), "Finite element modelling in engineering practice", Algor inc, USA, ISBN 0-9652806-0-8.*
17. *Timoshenko, S. and Goodier, J. N. (1951), "Theory of elasticity", Mcgraw-Hill, book Company, INC.*

AUTHORS PROFILE

Professor LM Masu holds BSc (Hons) Mech.Eng, MSc. Mech.Eng., PhD. (Leeds), PGDip. B Admin (UDW) and MBA (UFS). He is registered as Pr.Eng (ECSA), FSAIMechE, R Eng (K) and MIEK. Prof Masu has published 51 journal and 33 conferences articles, co-authored 1 book and 1 book chapter. He has a total of 38 years of academic experience, of which 27 years has been on academic managerial levels. In addition to this wealthy experience, Prof Masu has 4 years hands on industrial experience.

Dr PKNziu holds BSc (Hons), MTech and DTech inMechanical Engineering (VUT). He is registered as a candidate Eng.(ECSA) and Member (SAIMechE). He has published a total of 13 journal articles and presented 4 articles in international conferences. DrNziu has a total of 10 years academic experience in addition to $3^{1}/_{2}$ years hands onindustrial experience.